PHOTODISSOCIATION OF OZONE AT 248 nm AND VACUUM ULTRAVIOLET LASER-INDUCED FLUORESCENCE DETECTION OF O(¹D)

A. M. SARWARUDDIN CHOWDHURY*

*Laboratory of Molecular Photochemistry, Division of Material Science,
Graduate School of Environmental Earth Sciences,
Hokkaido University, Sapporo 060, Japan*

Ozone molecules, O_3, were photodissociated in the presence of N_2 at 248 nm (KrF laser) to $O(^1D) + O_2(^1\Delta)$. The $O(^1D)$ atoms were detected by generating vacuum ultraviolet laser-induced fluorescence (VUV LIF) for the $3s^1D^0 - 2p^1D$ transition at 115.2 nm. The 115.2 nm probe laser was generated by frequency tripling ($\omega_{VUV} = 3\omega$) of the 345.6 nm PTP dye laser in a Xe gas cell.

Keywords: Ozone; $O(^1D)$; tripling in Xe; vacuum ultraviolet laser-induced fluorescence; Doppler profile

INTRODUCTION

Our planet Earth's atmosphere is a big photochemical reactor, in which the light source is the Sun. Solar radiation not only heats our planetary atmosphere, but it also drives most of the photochemically initiated processes. For example, the photochemistry of oxygen species ($O_x = O_3$, O, O_2) is considerable [1–5]. Among the oxygen species, atmospheric ozone (trioxygen, O_3), is a delicate chemical

---

*Present Address: Department of Applied Chemistry and Chemical Technology, Dhaka University, Dhaka-1000, Bangladesh.

species, whose presence is principally a vital topic of stratospheric chemistry, although the smaller amounts in the troposphere also have important environmental implications [6, 7]. Chemical processes in the stratosphere are intimately connected with the phenomenon of the ozone layer in the $15-45$ km altitude regime. The significance of the ozone layer is twofold: on one hand it absorbs ultraviolet solar radiation at wavelengths below 300 nm, so that this biologically harmful radiation is prevented from reaching the Earth surface; on the other hand it dissipates the absorbed energy as heat, thereby giving rise to the temperature peak at the stratopause simply by dissociating ozone molecules [6, 8]. The startling discovery of the so-called 'Antarctic ozone hole' in the stratosphere in each Antarctic spring [1, 7] also depicts the importance of the O_x chemistry of our atmosphere. The source of O atoms above an altitude of 50 km is mainly from the photolysis of O_2 in the Herzberg I and Schumann– Runge continua [9, 10]. Thus, $O(^1D)$ forms naturally in the upper atmosphere by the photolysis of ozone, O_3 and oxygen, O_2, by sunlight in the UV and VUV regions (Fig. 1) [1, 10]. It has been recently narrated that the populations of superthermal $O(^1D)$ atoms in the earth's atmosphere are higher than that estimated [11]. The conservation of elemental O atoms in the O_2-O_3 cycle is also well known [1]. Therefore, studies on photodissociation of ozone at 248 nm (KrF laser) and vacuum ultraviolet laser-induced fluorescence detection of $O(^1D)$ at 115 nm, is of great environmental importance. Previous laboratory techniques used for this type of investigation involved bulk photochemical methods with gas chromatograph–mass spectrometry, pulsed photolysis resonance fluorescence, time-resolved atomic resonance spectroscopy, *etc.* [12–17]. However, the atomic absorption methods with a resonance lamp had ambiguity in the absorption coefficient for analysis. Thus, previous experiments are less reliable because of difficulties with the experimental approach. Therefore, in this work, ozone molecules, O_3, were photodissociated in the presence of N_2 at 248 nm (KrF laser) to yield $O(^1D)+O_2(^1\Delta)$. The vacuum ultraviolet laser-induced fluorescence (VUV LIF) method [18–20] was employed, to detect the O atoms in the ^1D state at 115.2 nm.
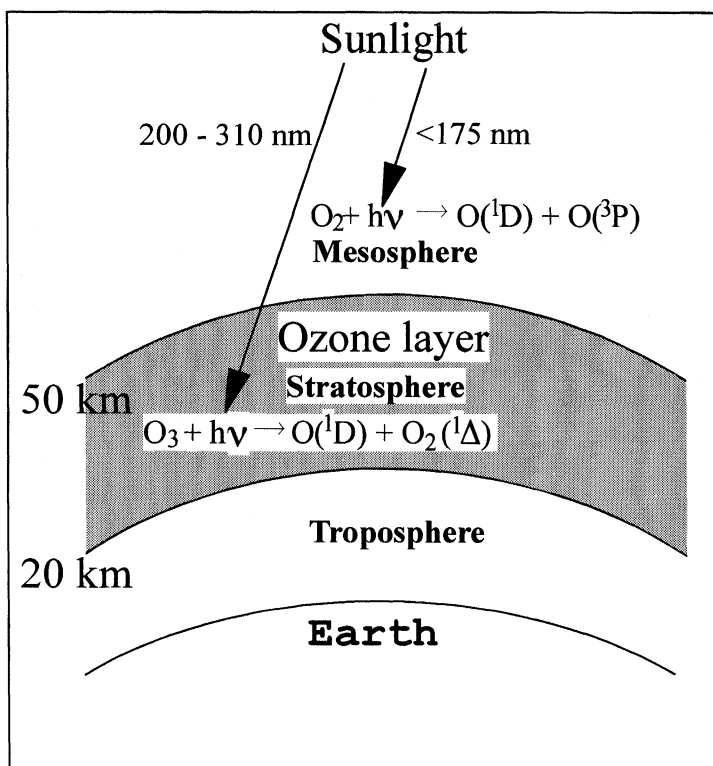
FIGURE 1 $O(^1D)$ forms naturally in the atmosphere by the photolysis of O_3 and O_2 by the sunlight in the UV and VUV region.

EXPERIMENTAL

A schematic illustration of the experimental apparatus for the photodissociation of ozone at 248 nm (KrF laser) and vacuum ultraviolet laser-induced fluorescence (VUV LIF) detection of $O(^1D)$ atoms at 115 nm is shown in Figure 2. The experiment was conducted in a photolysis-and-probe apparatus, using an excimer laser to dissociate the O_3 molecule in the presence of N_2 to produce slow $O(^1D)$ atoms as collisional products from the collisional reaction between generated superthermal $O(^1D)$ atoms and N_2 as collision
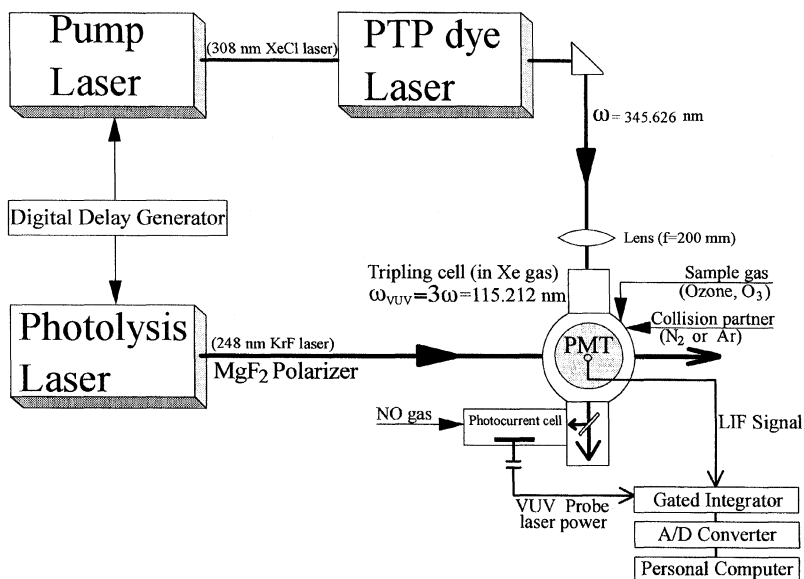
FIGURE 2   A schematic illustration of the experimental setup for the photodissociation of ozone at 248 nm KrF laser and vacuum ultraviolet laser-induced fluorescence (VUV LIF) detection of $O(^1D)$ atoms at 115 nm.

partner, and a dye laser system to probe the product $O(^1D)$ atoms by vacuum ultraviolet laser-induced fluorescence technique. The O_3 gas was slowly flowed through a stainless steel cell having an internal dimension of 80 mm and equipped with a port on each face. The photolysis, probe, and detector axes were mutually perpendicular. The gases used in the experiment was admitted into the cell through needle valves connected to the photolysis laser outlet arm and was exhausted through a port on the bottom face of the cell with a rotary pump and a liquid N_2 trap. In this experiment, O_3 and N_2 gas was used directly from an ozone reservoir (glass bulb) and cylinder. Absolute pressures in the reaction cell were measured by a capacitance manometer (MKS, Baratron 220). The photolysis wavelength was 248 nm, i.e., an KrF excimer laser (Lambda Physik, EMG 101 MSc, ~ 5 mJ/pulse, 10 Hz) was used as the photolysis source in generation of $O(^1D)$ atoms from photolysis of O_3. The 5 mm diameter laser beam entered the cell fitted with a 30 mm diameter quartz entrance window. The opposite face of

the cell was attached an arm fitted with a quartz window and a sample gas inlet.

The product $O(^1D)$ was probed by LIF, using a VUV laser beam at right angles to the photolysis laser. In fact, the $O(^1D)$ atoms were detected by generating vacuum ultraviolet laser-induced fluorescence (VUV LIF) for the $3s^1D^0 - 2p^1D$ transition at 115.212 nm. Thus, narrow-bandwidth VUV laser radiation is used to excite the fluorescence. A dye laser (Lambda Physik, FL 3002E) pumped by a XeCl excimer laser (Lambda Physik, LEXTRA 50, 308 nm, ~ 10 mJ/pulse, operated at 10 Hz) was used to generate coherent narrow-bandwidth VUV laser radiation of 115.212 nm by frequency tripling ($\omega = 3\omega$) in xenon gas (Fig. 3) [20, 21]. The dye laser output (PTP laser dye, p-terphenyl, $C_{18}H_{14}$, mol.wt. 230.31) was frequency-tripled in the Xe cell for ω wavelength of 345.636 nm. In this scheme, the fundamental laser beams are focused (quartz lens, $f = 200$ mm) into the nonlinear medium (e.g., Xe) of the tripling cell in order to increase the field strength and thus improve the nonlinear coupling between the input fields. The generated VUV light passed through a LiF window, propagated through a reaction cell, and was subsequently reflected into a VUV photocurrent cell of NO gas by another LiF plate. The intensity of the 115 nm probe laser light was thus monitored by a photoionisation current of nitric oxide gas (2 Torr).

The frequency tripling cell of xenon gas was a 200 mm-long stainless steel cylinder with a quartz inlet window and a LiF exit window and mounted onto one face of the reaction cell. Figure 3 shows a schematic diagram of the tripling cell (a) along with the frequency tripling process in Xe (b). Optimum VUV intensity was obtained as the beams were focused a few centimeters in front of the LiF exit window by reducing the effect of reabsorption of the generated VUV radiation while ensuring that the region of the beam focus remained wholly in the tripling cell. Absolute pressures in the tripling cell were measured by a capacitance manometer (Baratron 220), and the Xe gas pressure was 20 Torr.

A gas mixture containing the $O(^1D)$ source gas O_3, and N_2 was flowed slowly through a $80 \times 80 \times 80$ mm cubic reaction cell. O_3 molecules were dissociated at 248 nm by a polarized KrF laser. The dissociation light was focused by a CaF_2 lens ($f = 500$ mm) into the reaction chamber attached by a LiF window. The time delay between
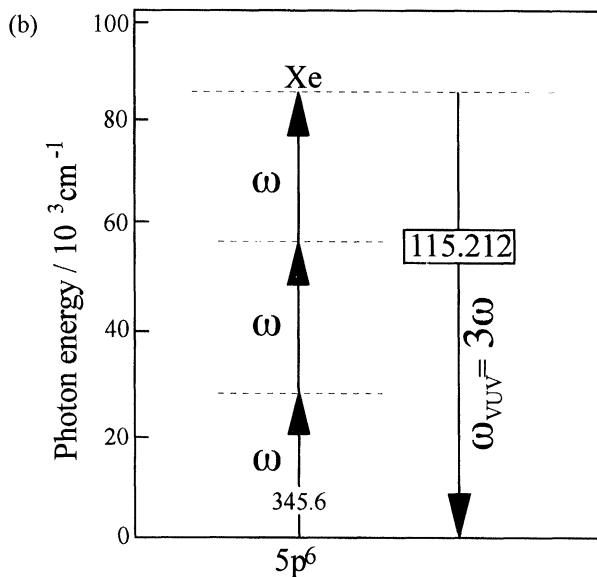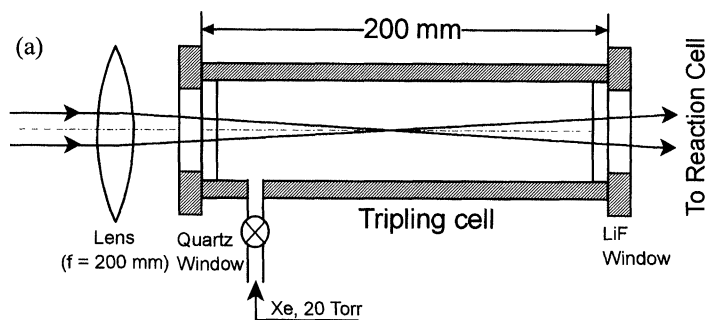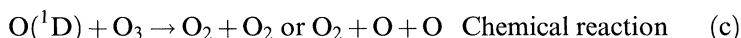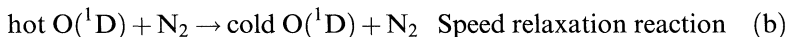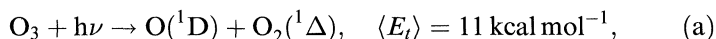
A. M. S. CHOWDHURY

FIGURE 3   The generation scheme of VUV laser light by frequency tripling in xenon, Xe. (a) Diagrammatic illustration of the tripling cell. (b) The generation scheme of 115 nm light by tripling ($\omega = 3\omega$) in Xe (Xe, 20 Torr). $O(^1D)$ atoms were detected by generating VUV LIF for the $3s^1D^0 - 2p^1D$ transition at 115.212 nm.

the dissociation and probe laser pulses was controlled by a digital pulse generator (Stanford Research, DG535), and the jitter of the delay time was less than 10 ns. The VUV LIF signal of $O(^1D)$ was detected at right angles to the propagation directions of both probe and dissociation laser light by a solar blind photomultiplier tube

(EMR, 541J-08-17) which had a LiF window and KBr photocathode that was sensitive only between 105 and 150 nm. This VUV LIF signals from the photomultiplier was then amplified in a preamplifier and averaged by gated integrators (Stanford Research, SR 250) which was interfaced to a laboratory computer. Ozone was prepared by passing ultrapure O_2 (Nihon Sanso, 99.9995%) through a commercial ozonizer and trapping the product on cooled silica gel. Ozone was degassed at liquid N_2 temperature and stored in a glass bulb. During the experiments, ozone was supplied to the reaction chamber through glass tubing and a polytetrafluoroethylene needle valve.

RESULTS AND DISCUSSION

The $O(^1D)$ atoms were obtained by the following reactions, initially, photodissociation of O_3 to get hot $O(^1D)$ atoms and then their subsequent collision with N_2 gives slow or cold $O(^1D)$ atoms.

$$O_3 + h\nu \rightarrow O(^1D) + O_2(^1\Delta), \quad \langle E_t \rangle = 11\, \text{kcal mol}^{-1}, \qquad \text{(a)}$$

$$\text{hot } O(^1D) + N_2 \rightarrow \text{cold } O(^1D) + N_2 \quad \text{Speed relaxation reaction} \quad \text{(b)}$$

$$O(^1D) + O_3 \rightarrow O_2 + O_2 \text{ or } O_2 + O + O \quad \text{Chemical reaction} \qquad \text{(c)}$$

where $\langle E_t \rangle$ is the average translational energy of the produced $O(^1D)$ atoms in the space fixed frame. The photodissociation laser light of 248 nm was generated by an excimer laser (Lambda Physik) operated with KrF mode for reaction (a). The translationally superthermal $O(^1D)$ atoms were mainly converted into slow $O(^1D)$ by the speed relaxation process by collisions with surrounding N_2 as according to reaction (b). In the upper atmosphere (stratosphere and mesosphere), N_2 remains as the paramount collider to deactivate superthermal $O(^1D)$ to cold $O(^1D)$ as the constituent of air is mainly $N_2(\sim 77\%)$. Let us come to the chemical reaction (c). As it has been known that the total reaction rate constant for $O(^1D) + O_3$ $(2.4 \times 10^{-10}\, \text{cm}^3$ molecule^{-1}s^{-1}) is around 10 times faster than that for $O(^1D) + N_2$ $(2.6 \times 10^{-11}\, \text{cm}^3\text{molecule}^{-1}\text{s}^{-1})$ [22] and also the partial pressure of O_3

is 500 times smaller than that of N_2 in this experiment, the possibility of the chemical reaction (c) is very much less, $i.e.$, the removal of $O(^1D)$ by the reaction process with O_3 is negligibly small.

It has been known that the visible and ultraviolet absorption spectrum of ozone consists of three diffuse bands, known as the Hartley band $^1B_2 \leftarrow \tilde{X}^1A_1$, 200–300 nm; the Huggins band $^1B_2 \leftarrow \tilde{X}^1A_1$, 300–360 nm; and the Chappius band $^1B_2 \leftarrow \tilde{X}^1A_1$, 450–850 nm; [23–25]. The Hartley band, which is essentially diffuse because of its dissociative nature, is the most intense of these bands [26]. There are two significant photodissociation paths for O_3 in the Hartley band: [1] $O_3 \rightarrow O(^1D) + O_2(a^1\Delta_g)$, $\Delta H = 92$ kcal mol^{-1} and [2] $O_3 \rightarrow O(^3P_j) + O_2(X^3\Sigma_g^-)$, $\Delta H = 24$ kcal mol^{-1} [26]. The dissociation channel [1], which has a quantum yield of 0.85–0.9, is referred to as a singlet channel [22, 27] and the quantum yield of the triplet channel [2] is 0.1–0.15 in the Hartley band [27]. Furthermore, for the photolysis reaction (a), from the low-lying singlet potential energy surfaces of O_3 along a dissociation coordinate $R(O_2-O)$, the ground state $O_3(\tilde{X}^1A_1)$, correlates asymptotically with $O(^3P_j) + O_2(^3\Sigma_g^-)$. An avoided crossing takes place between the $^1B_2$ and repulsive R^1A' state of O_3. This repulsive R^1A' potential surface correlates to $O(^3P_j) + O_2(^3\Sigma_g^-)$. Consequently, the adiabatic dissociation path of O_3 molecules excited to the $^1B_2$ surface leads to $O(^1D) + O_2(a^1\Delta_g)$ [26]. Therefore, at 248 nm, $O(^1D) + O_2(^1\Delta)$ were the main primary photodissociation products.

Decay of $O(^1D)$ atoms is shown in Figure 4. In fact, an initial increase in LIF intensity of $O(^1D)$ and then consecutive decay of $O(^1D)$, is observed in Figure 4, with the time delay after the photodissociation of O_3 at 248 nm with 1 Torr of N_2, when the probe laser wavelength is fixed at the center of the resonance line of $O(^1D)$ at 115.212 nm. The photodissociation products of O_3 at 248 nm were predominantly $O(^1D) + O_2(^1\Delta)$, and the initial formation of super-thermal $O(^1D)$ was substantially high. The LIF intensity of the $O(^1D)$ atoms decreases with delay time due to the collisional quenching process of the $O(^1D)$ atoms by N_2. At a delay time upto 4.8 µs, in Figure 4, the LIF intensity is decreasing, which means that all the hot $O(^1D)$ atoms produced by the photodissociation of O_3 are not still converted into cold $O(^1D)$ atoms, but has been converted to a considerable extent. Matsumi and Chowdhury [11] reported that at a
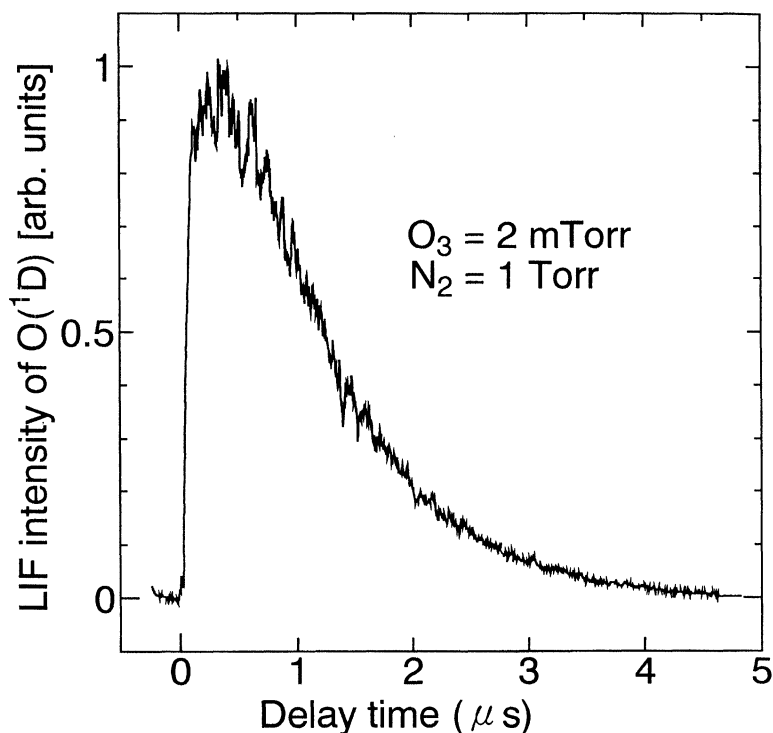
FIGURE 4   The decay curve of O(^{1}D). A plot of the LIF intensity of O(^{1}D) *vs* the delay time after the photodissociation of O_3 at 248 nm in the presence of N_2, when the probe laser wavelength is fixed at the center of the resonance line of O(^{1}D) at 115.212 nm. The pressures of O_3 and N_2 are 2 m Torr and 1 Torr, respectively.

long delay time around 5 µs, the LIF intensity becomes nearly asymptotic, *i.e.*, nearly all superthermal O(^{1}D) atoms produced by the photodissociation of O_3 are converted to cold O(^{1}D) atoms, which is in good agreement with this experiment. The decay of O(^{1}D) in Figure 4 for $t > 1$µs is in good agreement with the calculated value using the recommended rate constant [22] for O(^{1}D) + N_2 at 298 K. For comparison, the LIF intensity of O(^{1}D) with 1 Torr of Ar instead of N_2 is also plotted against delay time in Figure 5. At a delay time upto 4.8 µs, in Figure 5, the LIF intensity of O(^{1}D) atoms almost remains constant. That is very less speed relaxation of O(^{1}D) atoms takes place by collision with Ar. This indicates that N_2 is an efficient
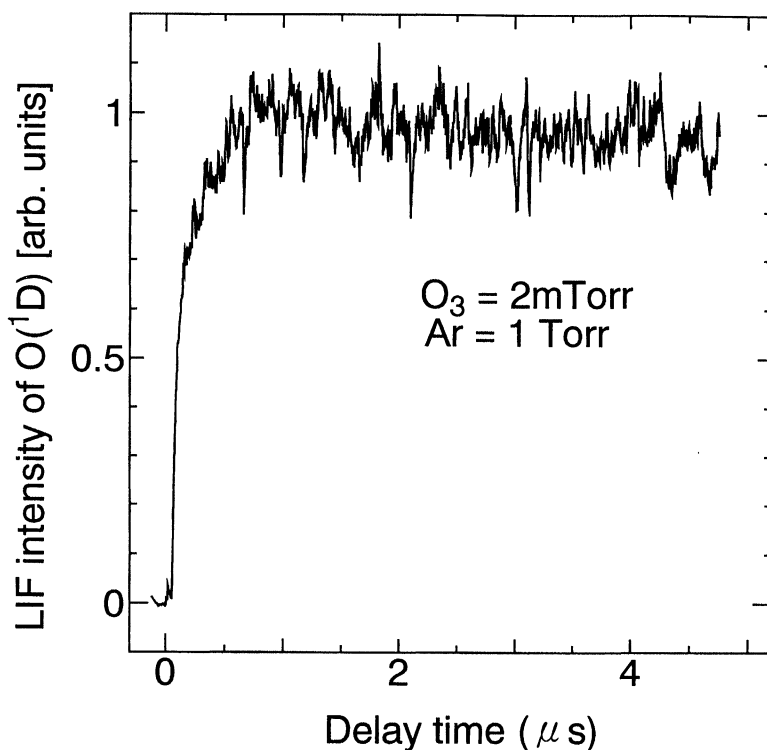
A. M. S. CHOWDHURY

FIGURE 5   A plot of the LIF intensity of O(^{1}D) *vs* the delay time after the photo-dissociation of O$_3$ at 248 nm in the presence of Ar, when the probe laser wavelength is fixed at the center of the resonance line of O(^{1}D) at 115.212 nm. The pressures of O$_3$ and Ar are 2 m Torr and 1 Torr, respectively. The LIF intensity of the O(^{1}D) atoms, in case of collision partner Ar, almost remains constant with delay time.

collider for the velocity relaxation of O(^{1}D) atoms and the decrease in the LIF intensity of O(^{1}D) atoms with N$_2$ is attributed to the speed quenching process and not to the escape of O(^{1}D) from the probing zone.

Figure 6 shows typical Doppler profiles of the O(^{1}D) atoms at various delay times, t = 100, 200, 300, 400, 500, 600, 800 and 1000 ns, when the O(^{1}D) atoms are produced by the photodissociation of O$_3$ at 248 nm KrF laser in presence of the N$_2$ molecules as bath gas. Doppler profiles at each delay time were taken for the optical configuration $k_p \perp E_d$. In fact, the resonance frequency of an O(^{1}D) atom exhibits a

$E_d \perp k_p$

Delay / ns

100 ns

200 ns

300 ns

400 ns

500 ns

600 ns

800 ns

1000 ns

-1 0   1

Doppler shift, $\Delta \nu$ (cm^{-1})
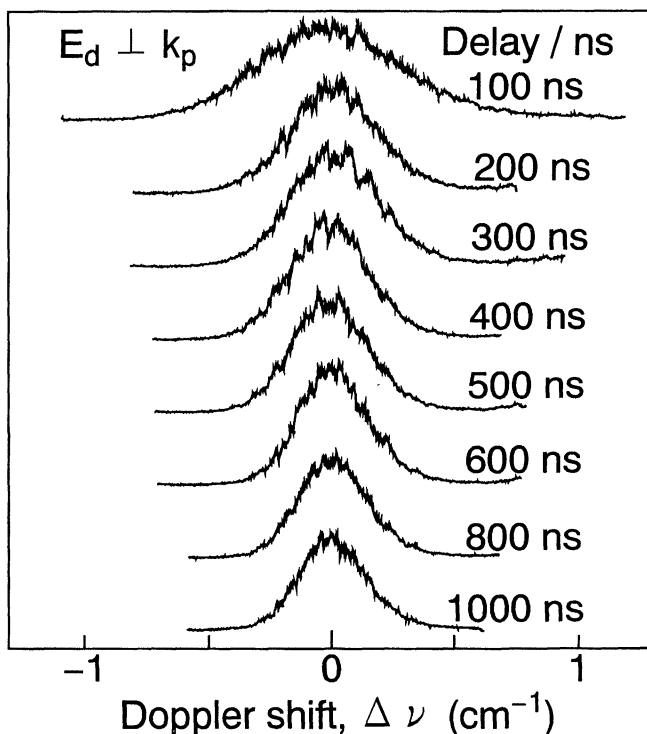
FIGURE 6   Doppler profiles for O(^{1}D) at various delay times ($t = 100-1000$ ns) between the photodissociation and probe laser pulses. The hot O(^{1}D) atoms are initially generated by the photodissociation of O$_3$ at 248 nm. The pressures of O$_3$ and N$_2$ are 2 mTorr and 1 Torr, respectively. The center wavelengths of the $3s^1D^0-2p^1D$ resonance transition is 86796.514 cm^{-1}. E_d is the direction of the electronic vector of the dissociation laser. k_p is the propagation direction of the probe laser.

Doppler shift $\Delta\nu = \nu_0 w/c$, where $w = v\cdot k_p$ is the component of the atom's velocity v along the unit vector k_p which describes the propagation direction of the probe laser, and ν_0 is the center frequency of the atomic transition. The probe laser beam propagated at right angles to the propagation direction of the dissociation laser k_d. The initial Doppler profile at 100 ns, in Figure 6, has a wide shape, which indicates the speed of the O(^{1}D) atoms. The width of the Doppler profiles becomes narrower with the increase in the delay times 200, 300, 400, 500, 600 ns, *etc.* (Fig. 6) indicating a reduction of the speed of O(^{1}D) atoms due to the increased number of collisions with N$_2$.

At long delay times, *e.g.*, 800, 1200, 2000 ns, *etc.*, the Doppler profiles of $O(^1D)$ become close to that of thermalized atoms, that is, becomes close to that of a Maxwell Boltzmann distribution at room temperature.

References

[1] Wayne, R. P., Chemistry of Atmospheres, (Oxford University Press, 1994).
[2] Stranges, D., Yang, X., Chesko, J. D. and Suits, A. G. (1995). *J. Chem. Phys.*, **102**, 6067.
[3] Miller, R. L., Suits, A. G., Houston, P. L., Toumi, R., Mack, J. A. and Woodke, A. M. (1994). *Science*, **265**, 1831.
[4] Chowdhury, A. M. S., Matsumi, Y. and Kawasaki, M. (1997). *Chem. Lett.*, **97**, 77.
[5] Toumi, R., Kerridge, B. J. and Pyle, J. A. (1991). *Nature*, **351**, 217.
[6] Warneck, P., Chemistry of the Natural Atmosphere, (Academic Press Inc., 1988).
[7] Goody, R., Principles of Atomospheric Physics and Chemistry, (Oxford University Press, 1995).
[8] Tachikawa, H., Hamabayashi, T. and Yoshida, H. (1995). *J. Phys. Chem.*, **99**, 16630.
[9] Hudson, R. D. and Carter, V. L. (1969). *Can. J. Chem.*, **47**, 1840.
[10] Okabe, H. (1995). Photochemistry of Small Molecules, (Wiley Interscience, 1978).
[11] Matsumi, Y. and Chowdhury, A. M. S. (1996). *J. Chem. Phys.*, **104**, 7036.
[12] Yamazaki, H. and Cvetanović, R. J. (1963). *J. Chem. Phys.*, **39**, 1902.
[13] Yamazaki, H. and Cvetanović, R. J. (1964). *J. Chem. Phys.*, **40**, 582.
[14] Streit, G. E., Howard, C. J., Schmeltekopf, A. L., Davidson, J. A. and Schiff, H. I. (1976). *J. Chem. Phys.*, **65**, 4761.
[15] Davidson, J. A., Schiff, H. I., Streit, G. E., McAfee, J. R., Schmeltekopf, A. L. and Howard, C. J. (1977). *J. Chem. Phys.*, **67**, 5021.
[16] Amimoto, S. T., Force, A. P., Wiesenfeld, J. R. and Young, R. H. (1980). *J. Chem. Phys.*, **73**, 1244.
[17] Force, A. P. and Weisenfeld, J. R. (1981). *J. Phys. Chem.*, **85**, 782.
[18] Chowdhury, A. M. S., Matsumi, Y. and Kawasaki, M. (1996). *Laser Phys.*, **6**, 865.
[19] Mack, J. A., Huang, Y., Woodke, A. M. and Schatz, G. C. (1996). *J. Chem. Phys.*, **105**, 7495.
[20] Chowdhury, A. M. S. and Kawasaki, M. (1996). *Laser Phys.*, **6**, 1175.
[21] Yamanouchi, K. and Tsuchiya, S. (1995). *J. Phys. B: At. Mol. Opt. Phys.*, **28**, 133.
[22] DeMore, W. B., Sander, S. P., Howard, C. J., Ravishankara, A. R., Golden, D. M., Kolb, C. E., Hampson, R. F., Kurylo, M. J. and Molina, M. J. (1980). Chemical Kinetics and Photochemical Data for use in Stratospheric Modeling No. 11, JPL Publication 94 – 26 (NASA, JPL, 1994).

[23] Shinha, A., Imre, D., Goble, J. H. Jr. and Kinsey, J. L. (1986). *J. Chem. Phys.*, **84**, 6108.
[24] Hay, P. J. and Dunning, T. H. (1980). *J. Chem. Phys.*, **67**, 2290.
[25] Hay, P. J., Pack, R. T., Walker, R. B. and Heller, E. J. (1982). *J. Phys. Chem.*, **86**, 862.
[26] Shamsuddin, S. M., Inagaki, Y., Matsumi, Y. and Kawasaki, M. (1994). *Can J. Chem.*, **72**, 637.
[27] Wayne, R. P. (1980). *Atmos. Environ.*, **21**, 1683.